Digital Communications Using Self-Phased Arrays

Leo D. DiDomenico, *Associate Member, IEEE,* and Gabriel M. Rebeiz, *Fellow, IEEE*

***Abstract*—A new technique for full duplex digital communications using adaptive phase conjugation is presented in this paper. The technique is based on mixing the RF signal to an IF where it can be easily processed, and filtering the phase of the IF signal to separate the geometry phase and message phase. The retrodirective array automatically tracks communicating platforms and transmits a directive return signal without the use of phase shifters. A 6-GHz microstrip retrodirective antenna array was built, together with the signal IF processing needed for full duplex operation. The measured *RCS* values of a linear six-element array are in good agreement with theory and results in a 0- to −5–dB *RCS* for angles up to $\pm 60^{\circ}$. The measured *RCS* values of a circular array are much flatter and are 0 to −5 dB up to $\pm 80^{\circ}$. Two-way digital communications at a baud rate of 78 kb/s was also demonstrated with $\mathrm{BER} < 10^{-6}$ for signal-to-noise ratios around 10 dB. The application areas are in high-performance digital mobile telecommunications for commercial and military applications.**

***Index Terms*—Adaptive beam forming, digital communications, phase conjugation, phase filtering.**

I. Introduction

In RECENT years, many RF systems have been designed with directed beam-forming capabilities for military and civilian communication applications. These systems are located on mobile platforms such as land vehicles, aircraft, and satellites. In addition, the platforms are operating in congesting environments that require multiple frequencies, code-division multiple access, or directed RF transmission in order to isolate the signals. In the case of directed transmission, phase shifters are used in order to perform narrow beam tracking. However, another technique exists. Developed circa 1950 [1]–[6] and performing the essential functions necessary for a directed RF link, it is called *phase conjugation* and has been used by many in the optics field for adaptive reconstruction of highly distorted optical signals [7] and, more recently, for RF communications [8], [9]. Phase conjugation at microwave and millimeter-wave frequencies is implemented using mixers as a substitute for materials with innate mixing properties, such as are found at optical frequencies [10].

The self-phased array idea (phase conjugation) is based on the arrangement shown in Fig. 1. In this figure, an unmodulated electromagnetic wave is traveling toward an antenna array. The distance to the nth array element is L_n and the wavelength is λ. The phase at the reference plane is $\phi_{\mathrm{Ref}} = 0$. It is easy to see that the round-trip phase, or return phase, is $\phi_{\mathrm{Return}} = 2(2\pi L_n/\lambda) + \Delta\phi_n$. If we wish to have constructive interference at the reference plane, then we may set the round-trip phase equal to zero for each element in the array. Therefore, the phase at the output of an array processing cell is $\phi_{\mathrm{Output}} = -\phi_{\mathrm{Input}} = -2\pi L_n/\lambda$. Hence, conjugation of an input RF signal is the requirement for constructive addition of a signal back at the reference plane. In addition, as long as this phase conjugation is done to within the *same additive constant* in phase at each of the antenna elements, then retrodirectivity will be achieved. A consequence that follows is that phase modulating all the array elements at the same time by a coding angle of $(0, \pi/2, \pi,$ etc.) rad will not impact the retrodirective property of the array.

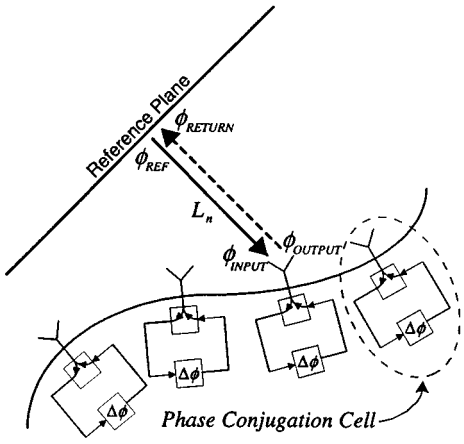

Fig. 1. Each phase processor modifies its input RF phase such that the total return signal will retroreflect and be sent back to its source.

A. Requirements

The main requirements placed on the prototype system were in functionality and versatility for experimenting purposes. In particular, the system was designed to have the following:

- directed transmission and omnidirectional receive antenna patterns for multiuser access;
- different frequency receiver and transmitter for higher RF isolation;
- scalable electronics capable of handling electrically large arrays;
- full duplex BPSK communications;
- conformal array.

The key points of the design will be given in the following sections.

II. Generating a Conjugated Signal

Various methods for producing phase conjugation and full duplexed communications are possible. Fig. 2 shows a simple

Manuscript received January 3, 2000. This work was supported by the Army Research Laboratory under a Federated Laboratories Fellowship and under a contract.

L. D. DiDomenico is with the Jet Propulsion Laboratory, Pasadena, CA 91104 USA (e-mail: leoddd@jpl.nasa.gov).

G. M. Rebeiz is with the Electrical Engineering and Computer Science Department, The University of Michigan at Ann Arbor, Ann Arbor, MI 48109-2122 USA (e-mail: rebeiz@umich.edu).

Publisher Item Identifier S 0018-9480(01)02431-0.

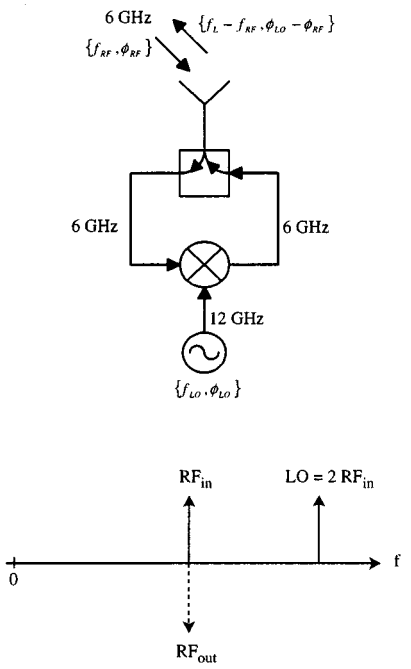

Fig. 2. Example of a phase conjugation cell that transforms the input RF energy to its phase conjugate.

phase conjugation cell [11], [12]. The cell consists of an antenna for transmitting and receiving a signal, and a mixer driven from a local oscillator (LO) at twice the RF frequency. The LO is common to the entire array. Note that the mixer's output frequency (typically called IF) is the same as the input frequency, and the mixer takes the difference of the phases of the RF and LO signals resulting in phase conjugation. Therefore, using normalized values of the RF and LO signals

$$v_{\mathrm{IF}}(t) = v_{\mathrm{RF}}(t)v_{\mathrm{LO}}(t) = \cos(\omega t + \phi)\cos(2\omega t). \quad (1)$$

This is expanded as a sum and difference in phase and then bandpass filtered (BPF) around the frequency ω as follows:

$$v_{\mathrm{RF,\,out}}(t) = v_{\mathrm{IF}}(t) \propto \Big[\cos(3\omega t + \phi) + \cos(\omega t - \phi)\Big] \xrightarrow{\mathrm{BPF}} \cos(\omega t - \phi). \quad (2)$$

Notice that the resulting output RF contains the negative of the phase of the input RF signal, thus achieving phase conjugation. Unfortunately, the method of using an LO at twice the RF frequency does not easily allow for full duplex communications since it is hard to process the phase at such high IF frequencies (>1 GHz). As a result, only retransmission of the original signal is practical, making this approach useful mostly for simple transponders.

Fig. 3 shows a phase conjugation cell that uses a low IF. An RF signal is received at a frequency and phase of $\{f_{\mathrm{RF1}}, \phi_{\mathrm{RF1}}\}$ and down converted to an IF via the first mixer with a LO at frequency f_{LO1}. The phase-locked loop (PLL) regenerates the IF signal to have a known amplitude and conjugated phase. It is assumed that $f_{\mathrm{LO1}} > f_{\mathrm{RF1}}$ so that phase conjugation can occur. The IF signal is upconverted to the RF using the upconversion mixer with $(f_{\mathrm{LO2}}, \phi_{\mathrm{LO2}})$, and the transmitted signal may be

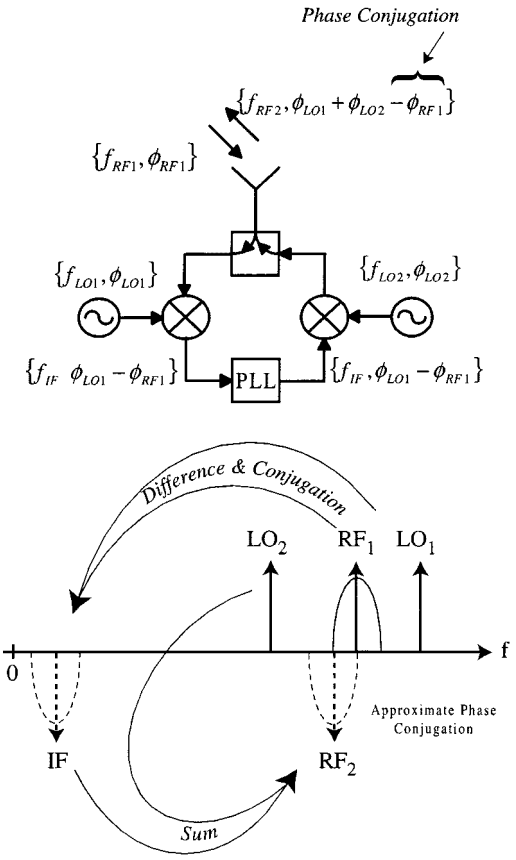

Fig. 3. Phase conjugation cell that uses an IF signal.

at a slightly different frequency from the input signal. The IF frequency is given by

$$v_{\mathrm{IF}}(t) = v_{\mathrm{RF1}}(t)v_{\mathrm{LO1}}(t) \quad (3)$$

and the resulting IF signal is filtered and regenerated by the PLL to give

$$v_{\mathrm{IF}}(t) \propto \Big[\cos\big((\omega_{\mathrm{RF1}} + \omega_{\mathrm{LO1}})t + \phi_{\mathrm{RF1}} + \phi_{\mathrm{LO1}}\big) + \cos(\omega_{\mathrm{IF}} + \phi_{\mathrm{LO1}} - \phi_{\mathrm{RF1}})\Big] \xrightarrow{\mathrm{BPF}} \cos(\omega_{\mathrm{IF}}t + \phi_{\mathrm{LO1}} - \phi_{\mathrm{RF1}}). \quad (4)$$

This signal then is upconverted to the RF in mixer 2 with the use of LO_2 and the *sum signal* is transmitted to preserve the conjugated phase.

Consider the receiver shown in Fig. 3. The received phase of the signal will change as function of time due to motion of the platforms communicating and the BPSK signaling. Hence, the signal phase has two components: message phase and geometry phase. The message phase is associated with the digital BPSK type signal and the geometry phase is associated with the platform dynamics. The geometry phase has frequency components in the range of 10–1000 Hz depending on the platform speed. The message phase has frequency components centered around 100 kHz or more, depending on the modulation technique. Therefore, it is possible, through data encoding, to separate the message phase and geometry phase in the frequency

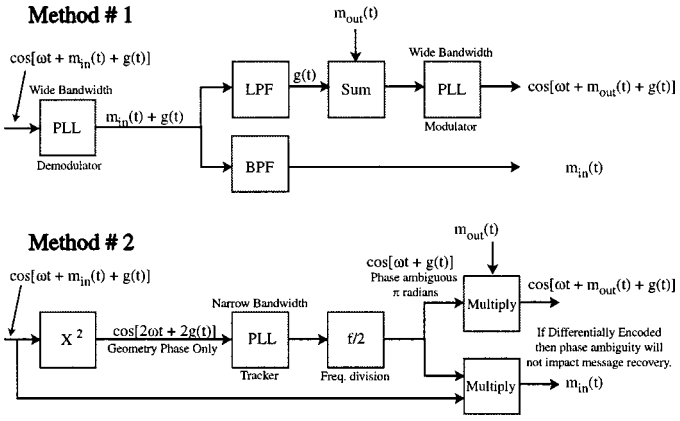

Fig. 4. Two different methods to do phase filtering. Method 2 was used in experiments.

domain. The geometry phase can then be used to create a regenerated (and conjugated) IF signal. This regenerated IF signal is then remodulated with a new message during the upconversion process by superimposing a new message phase on ϕ_{LO2}. The use of an IF frequency increases the system complexity, but allows access to the phase at a frequency where processing can easily be performed.

III. IF Processing Architecture

A. Phase Filtering Circuits

The use of an accurate IF phase filtering circuit is essential to the operation of the IF-based phase conjugation system. The circuit ensures that a regenerated carrier with zero phase error is obtained at the IF, and can be implemented using a simple squaring-type PLL. An attractive filtering method is the serial digital phase filter (SDPF) [13]–[16]. The SDPF is a type of PLL that does not require a voltage-controlled oscillator, and performs the phase-locked function with only logical operations. The SDPF uses no floating-point calculations, and can operate real time on the conjugated IF signal.

The basic steps necessary for phase filtering are shown in Fig. 4, although the actual implementation is based on digital techniques. Two methods are shown, and method 2 was chosen since it requires a narrow-band PLL. In both cases, a signal is processed that contains geometry phase and message phase $g(t)$ and $m_{\mathrm{in}}(t)$, respectively. The input message phase is then replaced by a new output message phase $m_{\mathrm{out}}(t)$, while the geometry phase is preserved.

B. Architecture

The prototype adaptive antenna array and communication system is based on the architecture shown in Fig. 5. This figure is read from the left- to right-hand side. The input to the system is an electromagnetic signal and is sampled at the receiver's antenna elements. After reception, low-noise amplifiers may be used to improve the system gain and noise figure. Each channel is downconverted using single-sideband (SSB) mixers that are from a common LO. The LO signal received at each mixer is matched in amplitude and phase. The IF signals generated in each channel are phase-conjugated versions of the input RF signals, and contains both the message phase and geometry phase. Next, a bandpass filtering operation is used to remove out-of-band noise, which may interfere with the SDPF operation.

Following the BPF, threshold detection is performed. This is essentially a one bit A-to-D conversion and the resulting signal is in the digital domain. It has no amplitude information and only phase information is retained. Since BPSK-type modulation is being used, a squaring process will remove the message phase information while preserving the geometry phase information. The squaring process is implemented using an edge detector. After edge detection, the signal in each channel is at twice the frequency and the phase of the IF carrier of the signal. Since the changes in phase at this stage are relatively slow (geometry phase), it is possible to use a PLL to lock to this edge-detected signal.

The outputs from all the IF PLLs are locked to the RF signal at each of the antenna elements. Each signal is then frequency divided using digital counters on the raw carrier and data recovery block of Fig. 5. However, the squaring process will force the IF signal at each channel to be ambiguous by π rad after being frequency divided. Each of the two states (zero or π) will have a probability of 1/2 of being asserted. This ambiguity is resolved using the recovered message phase. Each channel should ideally recover the same message phase, and if any of these recovered message signals is not in agreement with channel 1 (the reference channel), then the phase of the offending IF carrier is inverted. Hence, a comparison of the outputs of all the channels has to be undertaken, and this is done at the phase ambiguity correction (PAC) block.

Note, in order to compare the message phase of each channel, the IF signal must be sampled at the symbol modulation rate (around 100 kHz). The symbol clock is derived from another set of PLL circuits that are designed to pick out the frequency component, which is located at twice the symbol rate (around 200 kHz). This spectral component is a result of the modulation format of the message data. In particular, digital data from a $\Sigma - \Delta$ coder decoder (CODEC) was converted to Bi-ϕ format and then differentially encoded so that data statistics and π rad of phase ambiguity would not impact timing recovery. More details on the message encoding mechanism are given in [17].

After the PAC, raw-formatted differentially encoded Bi-ϕ data is present and all the regenerated phase-conjugated IF carriers are available. The digital signal that represents the IF carrier is said to be *synchronously ambiguous*. This means that there may be a phase error of zero or π rad across the entire array. However, all the channels have the same phase error and, therefore, the resultant IF carrier when upconverted will have a pattern that points back in the direction of the original source. Recall that phase conjugation must occur to within an additive phase constant across the array.

The message data is decoded and passed through a $\Sigma - \Delta$ CODEC for conversion to baseband data. While this is happening, a new message signal is also being passed through the CODEC and converted to nonreturn to zero (NRZ) type data. This data is then encoded into differential-Bi-ϕ and used to modulate the recovered IF carrier using the BPSK format. The resulting signal on each channel has the same output message

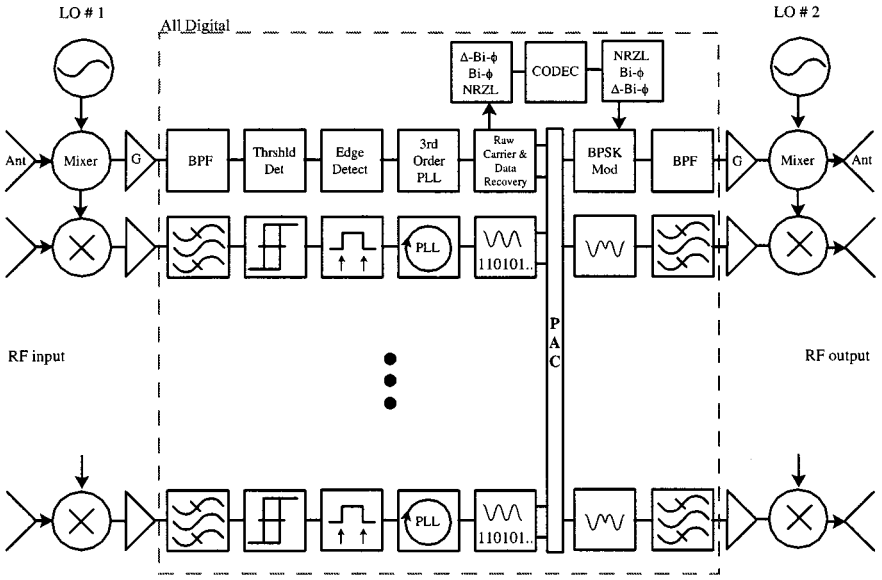

Fig. 5. Summary of the system.

information, m_{out}. These signal are filtered and upconverted to the RF frequency using the upper sideband of SSB mixers. The mixers are also driven from a single LO source, and is distributed with equal phase and amplitude. The signal may be amplified at the RF if necessary. Also, the transmit antennas are located at the same location as the receive antennas. The transmit frequency does not need to be the same as the receive frequency so that improved isolation may exist between the receiver and transmitter. This allows greater transmitter powers to be used without causing inadvertent feedback.

C. Implementation

The entire IF system shown in the dashed box of Fig. 5 has been implemented using a FLEX series field programmable gate array (FPGA) from Altera Corporation, Irvine, CA [17]. At the time of this paper's publication, it is possible to place several hundred of the processing channels in a single FPGA-type device. This represents a significant advantage and allows the size of the array to grow without concern over the real-estate needed for the IF processing.

IV. Measurements

The array measurements were made under laboratory conditions for both a single RF tone and a modulated BPSK signal of random data. The goal was to ensure that the array was capable of performing the retrodirective communications function while simultaneously separating out the geometry phase. Hence, no effort was spent on designing a low sidelobe array. In fact, the freedom of being able to place the individual antenna elements in arbitrary positions made the interelement spacing large enough to cause grating sidelobes for some of the arrays. For the following experiments, a six-element microstrip array on $\epsilon_r = 2.2$ Duriod with a thickness of 10 mil was used. The measured individual antennas show a -10-dB bandwidth of 50 MHz, centered at 5.9 (transmit) and 6 GHz (receive), respectively.

A. Pattern Synthesis Based on IF Phase Measurements

The antenna under test is placed on a rotating platform along with all the support electronics. Two small source antennas were located about 1-m distant from the retrodirective array. The source antennas were mounted on a linear track. The 1-m distance puts the transmit source in the Fresnel zone of the retrodirective array. One of the antennas is the BPSK modulated RF source at 5.99 GHz and the other antenna is a narrow-band RF noise source at 5.99 GHz with a bandwidth of about 60 MHz. The RF noise source was used for bit error rate (BER) analysis, and will be discussed in detail in the following section. The RF source antenna is a copolarized patch antenna similar to the type used in the retrodirective array. Both the source and receiver antennas had the E-plane in the horizontal plane.

In order to make the measurements at the IF stage (at 2 MHz), the signals from each of the channels was measured with a HP-54620A logic analyzer. The precise timing data of each IF channel was recorded, and the relative phase of each RF signal at each antenna element is, therefore, determined. To ensure accurate measured timing information, the BPSK modulation was turned off when phase measurements were made at the IF. In addition, the array was tuned to retransmit at an offset frequency of 10 MHz from the receive frequency with the use of $f_{\text{LO2}} = 5.99$ GHz. This is done in order to avoid coupling the output of the transmit antenna to the receive antenna.

The resulting antenna array pattern (AP) was synthesized according to the equation

$$\text{AP}(\mathbf{r}) = \sum_{\mathbf{n=1}}^{\mathbf{M}} \mathbf{a_n} e f_n(\mathbf{r'}, \hat{\mathbf{e}}) \mathbf{e^{j(k|r-r'_n|+\beta_n)}} \tag{5}$$

where the relative weighting a_n were set to one, the source positions $\mathbf{r'}$, orientation vector of each element $\hat{\mathbf{e}}$, and impressed phases β_n were measured. The normalized element

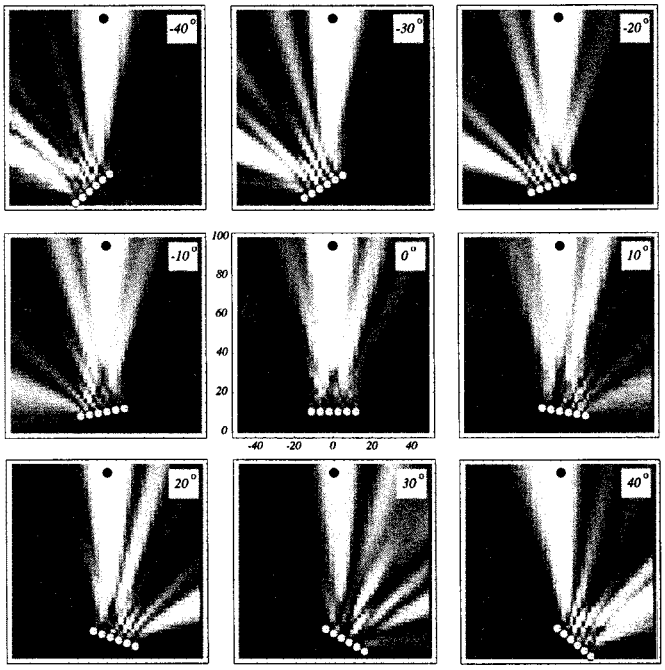

Fig. 6. Calculated linear APs based on the measured retransmitted IF phase at each of the antenna elements.

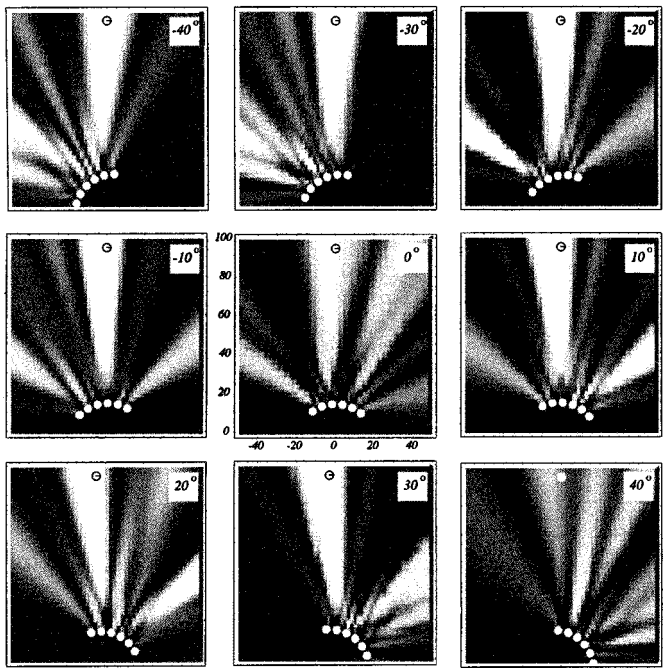

Fig. 7. Calculated circular sector APs based on the measured retransmitted IF phase at each of the antenna elements.

factor $ef_n(\mathbf{r}', \hat{\mathbf{e}})$ for a copolarized E-plane cut of a microstrip antenna is

$$\mathrm{EF} = \cos\left(\frac{kl}{2}\sin\theta\right) = \cos\left(\frac{\pi}{2\sqrt{\epsilon_r}}\sin\theta\right) \qquad (6)$$

where $k = 2\pi/\lambda$, l is the resonance length of the patch antenna (typically $\lambda_d/2$), ϵ_r is the dielectric constant, and θ is the angle from the normal to patch antenna. Note, that no far-field approximations were used to evaluate the sum in (5).

Fig. 6 shows the magnitude of the retransmitted power from the retrodirective linear six-element 0.9λ interelement spaced array as a function of position of the source (a small circular dot at the top of each image). The orientation of the retrodirective array is shown at the bottom of each image. Note how the retransmitted main beam is always pointing back in the direction of the source. As expected, the grating lobes are observable at large scanning angles and could have been suppressed with an interelement spacing of 0.6λ.

Fig. 7 shows the same type of patterns for a circular arc of radius 20 cm with interelement angular spacing of 15°. Patterns are shown for various angles of rotation of the retrodirective array. Again, the main beam is seen to track the source. In this figure, there are also undesired grating lobes. The undesired sidelobes were expected and are entirely due to the spacing of the array elements. The last image shows a loss of signal due to loss of phase lock when the input signal to the array had its SNR drop below the minimum acceptable value for proper operation of the PLL.

B. Far-Field Pattern and RCS Measurements

Far-field measurements were done in the anechoic chamber and the bistatic *RCS* measurements were made at the RF. Actually, these measurements were very close to monostatic, but were limited from being true monostatic measurements by experimental setup. The adaptive antenna array was configured for offset frequency operation. The center frequency of the input signal to the adaptive array was 5.90 GHz and the retransmitted signal from the array was at 6.00 GHz, so that an isolation frequency of 100 MHz between receive and transmit was utilized. The minimum offset frequency that would still allow proper operation was 10 MHz and is due to transmitter–receiver feedback.

The source antenna gain is 28 dB with a maximum power level of 17 dBm and the bistatic receive antenna gain is 23 dB. These antennas are co-located with 0.5-m separation. The source signal is BPSK modulated with a 78.125-kHz symbol rate or random data. The range from the source to the adaptive antenna array is 15 m and the corresponding space loss is around 72 dB. Hence, a maximum signal level of about -27 dBm is seen at the adaptive antenna array. In addition, another 60 dB of variable attenuation is placed at the source for minimum sensitivity measurements. The adaptive antenna functioned well with received power levels as low as about -59-dBm per element (see Section IV-C).

1) Linear Array Measurements: Fig. 8 shows the linear array in the anechoic chamber during testing. The array was tested along the E-plane cut with horizontal polarization. The linear array measurements consisted of three patterns: two bistatic measurements (with and without modulation) and one standard antenna pattern. The standard antenna pattern was based on a corporate feed arrangement to the array elements using a commercial six-way divider. This measurement was used as a reference against which to compare the bistatic adaptive measurements. Two 50-Ω terminated dummy antenna elements were located at each end of the array for matching, and to act as probes to measure the field strength of the received and transmitted signals via a spectrum analyzer.

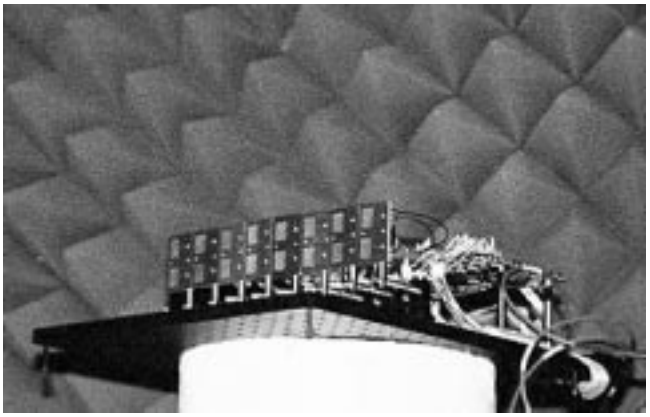

Fig. 8. Configuration of the antenna array used in the linear-array response measurements.

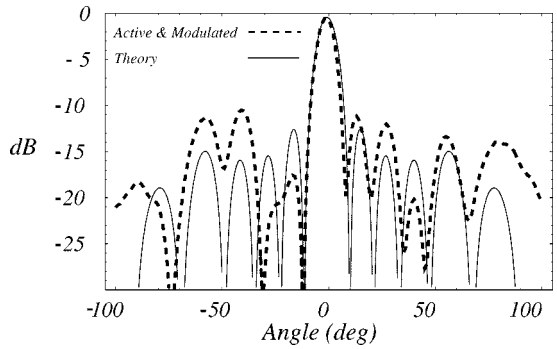

Fig. 9. Antenna pattern of the linear array when all the elements are coherently combined. Theoretically expected response are also shown.

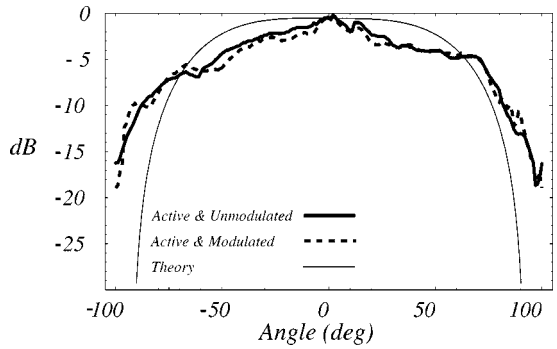

Fig. 10. Normalized *RCS* of the linear array when sending and receiving a tone, and a modulated signal. The theoretically expected response is also shown.

Fig. 9 shows the results of the standard pattern measurements. The pattern shows the characteristic main beam of the linear array with sidelobes at 13 dB down from the central beam. The 3-dB beam width is 8°, and agrees well with calculations.

The bistatic measurements, with the active antenna used as a phase-conjugating retrodirective array, are shown in Fig. 10, both with and without modulation. It is seen that retrodirectivity is evident even with a digital communications link, and that the six-element array results in a 0–5-dB *RCS* for angles up to ±60°.

The *RCS* measurements are consistent with the theory of phase conjugating devices like corner cubes [19] and are also in good agreement with the power falloff expected from to 90°).

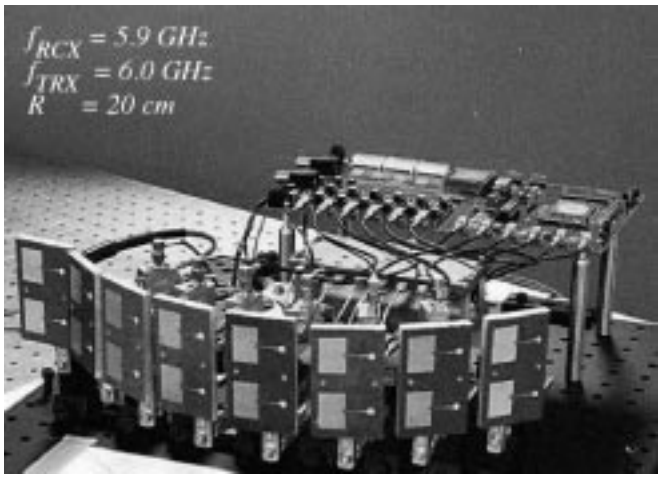

Fig. 11. Configuration of the antenna array used the circular sector array response measurements. The elements at the edge are used for power reference and are not part of the active array.

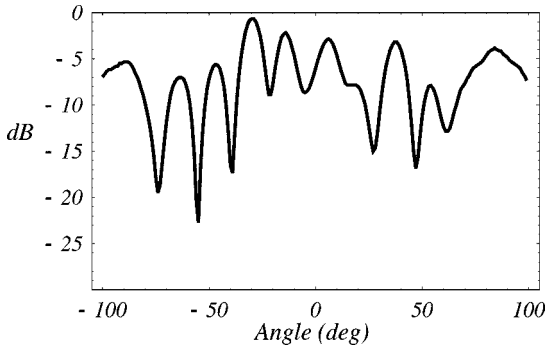

Fig. 12. Antenna pattern of the circular sector array when all the elements are coherently combined.

This is due to the element pattern and edge diffraction at the boundary of the array. Also, the theory is based on a continuous aperture, whereas the measurements is based on a six-element array. The *RCS* measurements were also done with both the antenna and its supporting structure (Fig. 8) and these signals can cause constructive or destructive interference.

2) Circular Array Measurement: The data was again taken under active and passive modes for an antenna in the form of a circular arc. Fig. 11 shows the configuration used in the anechoic chamber. The radius of the arc is 20 cm and the angular separation is 15° between the antenna elements. Fig. 12 shows the results of the standard pattern measurements using a six-way power divider with equal phase. The AP is not well defined, in fact, it is almost a random pattern. This shows that circular arrays need to be very carefully fed if used in a standard configuration.

Fig. 13 shows the response of the circular retrodirective array, and it is the same for both modulated and unmodulated signals. The *RCS* response is flatter than for the linear array. This is to be expected since the circular array has a greater effective area in the direction of the bistatic RF source at large angles of incidence. Even at 90°, the array still has half of its antenna elements visible at the RF source position. The results of the circular array shows that retrodirective antennas can be placed on curved communication platforms (such as antenna towers,

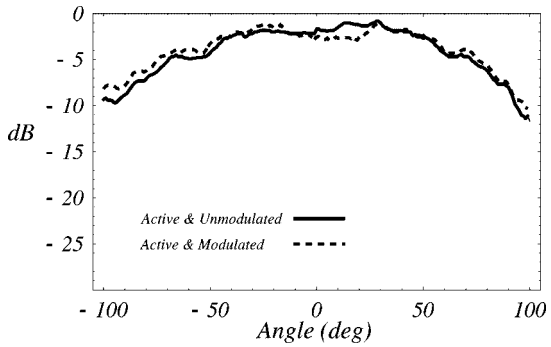

Fig. 13. Normalized *RCS* of the circular sector array when sending and receiving a tone and modulated signal.

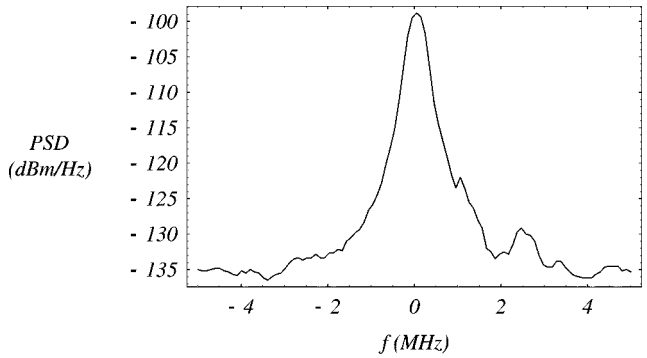

Fig. 14. PSD of the IF signal measured with the noise marker function of the HP-8592L spectrum analyzer.

wings, or fuselage) and still maintain excellent transmit patterns and *RCS*.

C. Symbol Errors

The BERs were measured by a direct comparison of the source data to the recovered data. The error pulses were collected using a computer-controlled universal counter that partitioned time into 30-s measurement intervals. The inputs to the adaptive array were a noise signal of 60-MHz span about the signal center frequency of 5.9 GHz and the actual signal information bearing signal. The noise power levels were flat over the 60-MHz span and the noise power is controllable for each BER experiment.

The peak of the power spectral density (PSD) of the *data signal* was maintained at -99 dBm/Hz for simplicity. For each experiment, the noise power was changed. There were a total of 45 different 30-s error measurements using different noise PSDs. The purpose of dividing time into 30-s subintervals for each noise PSD is to allow observation of burst errors in the recovered data. Burst errors are large numbers of errors grouped in a relatively short time, and are highly correlated to each other. Burst errors may be due to a variety of causes, including man-made electromagnetic interference (EMI), or PLL cycle slip, which is typical of digital communication systems.

The PSD of the signal is shown in Fig. 14. The measured -3-dB bandwidth of the IF phase signal is 410 kHz and is a result of a 78.125-kb/s symbol rate that is encoded with a differential Bi-phase format and upconverted without any filtering. In addition, the noise bandwidth, as defined by the IF analog amplifiers bandwidth, was measured to be about 50 MHz. This is less than the bandwidth of the noise sourced from the noise source. Therefore, all calculations were made with white-noise PSDs, i.e., constant power level PSDs. The SNR was calculated by

$$\mathrm{SNR} = \left(\frac{\rho_S}{\rho_N}\right)\left(\frac{\Delta f_S}{\Delta f_N}\right) \tag{7}$$

where ρ_S and ρ_N are the PSDs of the signal and noise, and Δf_S and Δf_N are the bandwidths of the signal and noise, respectively.

Based on the above discussion, the BER was measured and plotted for 100 different experiments each at a different

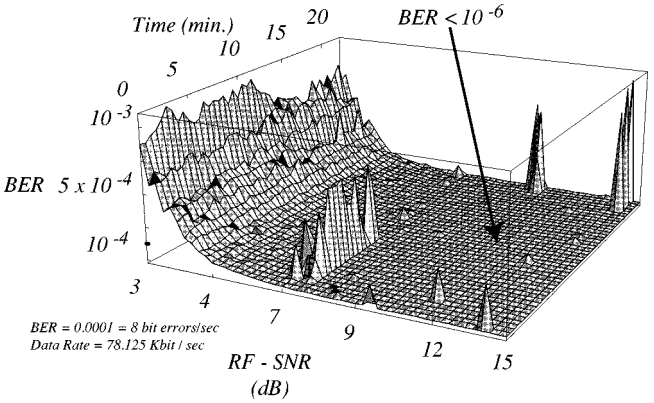

Fig. 15. BER plot shows the effects of burst noise. The angle between source and receiver was 0° and the effective distance was controlled by electronic attenuators.

SNR. The experiments were conducted with an offset-frequency phase-conjugation-based communications link in two directions, i.e., full duplex. Each of the 100 experiments took 22.5 min to perform with 45 subintervals at 30-s per interval. Hence, at 78.125 kb/s, each 30-s subinterval tested 2 343 750 bits and each of the different SNR level had in excess 100×10^6 bits of compact disk (CD) quality random audio data tested.

Fig. 15 shows the BER best for noisy signals. It is observed that for $\mathrm{SNR} > 9$ dB, the BER was less than 10^{-6} for about 98% of the time. The other 2% of the time, the BER was adversely affected by burst noise. This noise could have been a result of man-made EMI, but was most likely a result of the receiver losing lock temporarily due to cycle slips in the PLL. Such errors could be removed by making the PLL circuits synchronous instead of asynchronous, as in the electronics developed in this project. In any event, a BER of 0.0001 is equivalent to 8-b errors per second at a baud rate of 78.125 kb/s, and was more than sufficient for excellent voice quality digital audio applications. In fact, the audio was able to be discerned by the human sense of hearing with input noise power levels of -120 dBm/Hz at SNRs of about 2 dB. This corresponds to a BER of greater than 0.01 or about 800-b errors per second. Hence, the voice audio communications were proven to be reasonably robust even without any error correction coding.

V. Conclusions

A design for a self-phased retrodirective adaptive antenna array capable of full duplex digital communication has been proposed and tested in this paper. Although more sophisticated system architectures can be devised, the fundamental principle of mixing the RF signal to an IF where it can be easily processed, and filtering the phase of the IF signal to separate the geometry phase and the message phase for full duplex operation, remains unchanged. The system is limited to small frequency changes, i.e., Δf, due to Doppler shifts. However, for many narrow-band applications, this is satisfactory.

The measured data show that the transmit antenna pattern does self-phase and become retrodirective when the full duplex communication function was being utilized. The measured *RCS* values of a linear six-element array are in good agreement with theory and results in a 0- to -5-dB *RCS* for angles up to $\pm 60^{\circ}$. The measured *RCS* values of a circular array are much flatter and are 0 to -5 dB for angles up to 80°. Two-way digital communications was also demonstrated with $\mathrm{BER} < 10^{-6}$ for SNRs around 10 dB. Further improvements should be possible with the addition of error correction coding and a fully synchronous design.

Acknowledgment

The authors would like to thank Dr. B. Perlmann, Communications and Electronics Command (CECOM), (formerly of the Army Research Laboratory, Fort Monmouth, NJ), Dr. B. Wallace, Army Research Laboratory, Fort Monmouth, NJ, and Dr. E. Burke, Army Research Laboratory, Fort Monmouth, NJ, for their support of this paper.

References

[1] L. C. Van Atta, "Electromagnetic reflector," U.S. Patent 2 908 002, 1955.
[2] E. D. Sharp and M. A. Diab, "Van Atta reflector array," *IRE Trans. Antennas Propagat.*, vol. AP-8, pp. 436–438, Apr. 1960.
[3] M. I. Skolnik and D. D. King, "Self-phasing array antennas," *IEEE Trans. Antennas Propagat.*, vol. AP-12, pp. 142–149, Feb. 1964.
[4] C. Y. Pon, "Retrodirective array using the heterodyne technique," *IEEE Trans. Antennas Propagat.*, vol. AP-12, pp. 176–180, Feb. 1964.
[5] S. N. Andre and D. J. Leonard, "An active retrodirective array for satellite communications," *IEEE Trans. Antennas Propagat.*, vol. AP-12, pp. 181–186, Feb. 1964.
[6] E. M. Rutz-Philipp, "Spherical retrodirective array," *IEEE Trans. Antennas Propagat.*, vol. AP-12, pp. 187–194, Feb. 1964.
[7] R. K. Tyson, *Principles of Adaptive Optics*. New York: Academic, 1991.
[8] S. L. Karode and V. F. Fusco, "Self-tracking duplex communication link using planar retrodirective antennas," *IEEE Trans. Antennas Propagat.*, vol. 47, p. June, June 1999.
[9] Y. Chang, H. R. Fetterman, I. L. Newberg, and S. K. Panaretos, "Microwave phase conjugation using antenna arrays," *IEEE Trans. Microwave Theory Tech.*, vol. 46, pp. 1910–1919, Nov. 1998.
[10] A. Yariv, *Optical Electronics*, 4th ed. Philadelphia, PA: Saunders, 1991.
[11] C. Pobanz and I. Itoh, "Time varying active antennas, circuits and applications," Ph.D. dissertation, Univ. California at Los Angeles, Los Angeles, CA, 1997.
[12] ——, "A microwave noncontact identification transponder using subharmonic interrogation," *IEEE Trans. Antennas Propagat.*, vol. 43, pp. 1673–1679, July 1995.
[13] W. H. Lee, E. V. Harrington, and D. B. Cox, "A new integrated-circuit digital phase-locked loop," in *Nat. Aerospace Electron. Conf.*, 1975, pp. 377–383.
[14] D. B. Cox, E. V. Harrington, W. H. Lee, and W. M. Stonestreet, "Digital phase processing for low-cost omega receivers," *J. Inst. Navigat.*, vol. 22, no. 3, pp. 221–234, 1975.
[15] D. H. Wolaver, *Phase Lock Loop Circuit Design*. Englewood Cliffs, NJ: Prentice-Hall, 1991.
[16] R. E. Best, *Phase Locked Loops*, 3rd ed. New York: McGraw-Hill, 1997.
[17] L. D. DiDomenico, "Mobile digital communications using phase conjugating arrays," Ph.D. dissertation, Dept. Elect. Eng., Univ. Michigan at Ann Arbor, Ann Arbor, MI, 1999.
[18] C. Balanis, *Antenna Theory*. New York: Wiley, 1992.
[19] N. Levanon, *Radar Principles*. New York: Wiley, 1988.

Leo D. DiDomenico (A'90) received the B.A. degree in physics and B.S. degree in electrical engineering, and M.S.E.E. degree from Rutgers, The State University of New Jersey, Piscataway, NJ, in 1990 and 1994, respectively, and the Ph.D. degree in electrical engineering from The University of Michigan at Ann Arbor, in 1999. His doctoral research concerned the field of electromagnetics and self-phased adaptive antenna arrays for digital mobile communications, tracking radar, or self-tracking directed-energy systems.

From 1990 through 1991, he was with TRW Space and Defense Systems, where he was involved with high-power optical systems characterization. He then joined the Army Research Laboratory, Ft. Monmouth, NJ, where he helped develop novel antennas and beamforming technology, including superconducting antennas, ceramic phase-shifter technologies, and RF-based personal-identification tagging systems. From 1995 to 1999, he was with both The University of Michigan at Ann Arbor and the Army Research Laboratory, Adelphi, MD, where he was involved with adaptive antenna arrays. He is currently with the NASA Jet Propulsion Laboratory, California Institute of Technology, Pasadena, where he is involved with designs and advanced concepts for radars and other technologies. His professional interests are in researching advanced concepts and designs in electromagnetic systems for aerospace applications, including radar, communications, remote sensing, and directed-energy electromagnetic propulsion or power transmission. He also enjoys investigating theoretical contemporary physics.

Gabriel M. Rebeiz (S'86–M'88–SM'93–F'97) received the Ph.D. degree in electrical engineering from the California Institute of Technology, Pasadena, in 1988.

In September 1988, he joined the faculty of The University of Michigan at Ann Arbor, and became a Full Professor in May 1998. He has been a Visiting Professor at Chalmers University of Technology, Göteborg, Sweden, Ecole Normale Superieur, Paris, France, and Tohoku University, Sendai, Japan. His research interests are in applying micromachining techniques and microelectromecanical systems (MEMS) for the development of novel components and subsystems for wireless communication systems. He is also interested in Si/GaAs radio-frequency integrated-circuit (RFIC) design for receiver applications, and in the development of planar antennas and microwave/millimeter-wave front-end electronics for applications in millimeter-wave communication systems, automotive collision-avoidance sensors, monopulse tracking systems, and phased arrays.

Prof. Rebeiz was the recipient of the 1991 National Science Foundation Presidential Young Investigator Award and the 1993 URSI International Isaac Koga Gold Medal Award for Outstanding International Research. He was also the recipient of the 1995 Research Excellence Award presented by The University of Michigan at Ann Arbor. Together with his students, he was the recipient of Best Student Paper Awards of the IEEE Microwave Theory and Techniques Society (IEEE MTT-S) in 1992 and 1994–1998, and the IEEE Antennas and Propagation Society (IEEE AP-S) in 1992 and 1995. He was the recipient of the 1990 Journess Internationales de Nice Antennas (JINA'90) Best Paper Award. He is also the recipient of the 1997 Electrical Engineering and Computer Science (EECS) Department, The University of Michigan at Ann Arbor, Teaching Award and the 1998 College of Engineering Teaching Award. He was selected by The University of Michigan at Ann Arbor's EECS students as the 1997–1998 Eta Kappa Nu Professor of the Year. In June 1998, he was the recipient of the Amoco Foundation Teaching Award, presented yearly to one (or two) faculty members of The University of Michigan at Ann Arbor for excellence in undergraduate teaching.